# ICES REPORT 10-29

**July 2010**

# Numerical Methods for Smooth and Crystalline Mean Curvature Flow

**by**

A. Oberman, S. Osher, R. Takei, and R. Tsai


**The Institute for Computational Engineering and Sciences**
The University of Texas at Austin
Austin, Texas 78712

*Reference: A. Oberman, S. Osher, R. Takei, and R. Tsai, "Numerical Methods for Smooth and Crystalline Mean Curvature Flow", ICES REPORT 10-29, The Institute for Computational Engineering and Sciences, The University of Texas at Austin, July 2010.*

# NUMERICAL METHODS FOR SMOOTH AND CRYSTALLINE MEAN CURVATURE FLOW

ADAM OBERMAN, STANLEY OSHER, RYO TAKEI, AND RICHARD TSAI

Abstract. We present two numerical methods for planar anisotropic mean curvature flow. The methods are based on the variational approach of Almgren, Taylor and Wang, and Chambolle. Our approach uses the Split-Bregman method for total variation minimization. In the crystalline anisotropy case, we derive and prove an algorithm for a corresponding polyhedral shrinkage (or soft thresholding) problem. In the smooth anisotropy case, the Split Bregman algorithm is used as an approximation to an inverse scale space flow and resembles diffusion generated motion by anisotropic curvature. Numerical results are presented.

## 1. Introduction

We study numerical methods for the time evolution of a closed planar curve $C(t)$ with normal velocity equal to its anisotropic mean curvature. The motion is the gradient flow of the anisotropic perimeter

$$\mathcal{E}_\phi(C) = \int_C \phi(\hat{n})\, ds.$$

Here, $\hat{n}$ is the unit outer normal to the curve $C$ and $ds$ is the arc-length measure. We assume $\phi$ is a convex, even, positively 1-homogeneous function, with $a(x) \leq \phi(x) \leq A(x)$ for all $x \in \mathbb{R}^2$.

The motion is a natural generalization to the well known (isotropic) mean curvature flow, or the curve-shortening flow, where the curve evolves to minimize its length

$$\mathcal{E}(C) = \int_C |\hat{n}|\, ds$$

We will consider separately two classes of anisotropy: smooth and crystalline. The latter is of interest, for example, in crystal growth [Gur93].

### 1.1. Motion of level sets by mean curvature.

One of the earliest successful numerical algorithm for isotropic mean curvature flow appeared in the article of Osher and Sethian [OS88]. Their idea is to represent the curve $C(t)$ as the zero level set of an auxiliary function $u(x,t)$, and to evolve this function by a degenerate elliptic Partial Differential Equation (PDE)

$$\frac{\partial u}{\partial t} = |\nabla u| \operatorname{div} \frac{\nabla u}{|\nabla u|}. \tag{1}$$

*Date*: May 12, 2010.

2000 *Mathematics Subject Classification.* subject class.

This PDE was subsequently analyzed in the viscosity solutions framework, by Evans and Spruck [ES91], and Chen, Giga and Goto [CGG91]. Monotone, convergent finite difference schemes for the mean curvature motion PDE were later discovered by Catte, et al. [CDK95] and Oberman [Obe04]. See also [DDE05] for finite element method implementations. The method of [Cha04] used Total Variation Minimization to numerically approximate the variational interpretation of the motion.

1.2. **Motion by anisotropic mean curvature.** We first describe the anisotropic analogue of (1). The *$\phi$-normal* to the curve is given by

$$\hat{n}_\phi = \nabla\phi(\hat{n})$$

where $\hat{n}$ is the unit normal to the curve. Then the anisotropic curvature of the curve is given by

$$\kappa_\phi = -\operatorname{div} \hat{n}_\phi$$

(or is an element of $\operatorname{div} \hat{n}_\phi$ whenever $\phi$ is not smooth). Noting that $\nabla\phi$ is homogeneous of degree 0, we follow the definition of [ATW93] and [Gig06] by evolving according to

$$\frac{1}{|\nabla u|}\frac{\partial u}{\partial t} = -\kappa_\phi = \operatorname{div} \nabla\phi(\nabla u) \tag{2}$$

which corresponds to the evolution with velocity $\kappa_\phi$ along the Euclidean normal to the surface.

*Remark.* There is more than one definition of this type of anisotropic curvature motion in the literature. The definition of anisotropic motion by mean curvature used by [Cha04] is derived in [NP07]:

$$\frac{\partial u}{\partial t} = \phi(\nabla u) \operatorname{div} \nabla\phi(\nabla u). \tag{3}$$

This definition assumes that the surface evolves with velocity $\kappa_\phi$ along the $\phi$-normal. In the case of smooth anisotropies, the PDE (3) is well-posed in the viscosity sense. It has been shown that Wulff shape is preserved under such evolution, with a rate $\sqrt{1-2t}$. It is not obvious that either (2) or (3) is more natural. We point out that either equation can be approached by our numerical methods.

For smooth anisotropy, (2) can be written as

$$\frac{\partial u}{\partial t} = (\gamma(\theta) + \gamma''(\theta))|\nabla u| \operatorname{div} \frac{\nabla u}{|\nabla u|} \tag{4}$$

where, $\phi(x_1, x_2) = \gamma(\theta)\sqrt{x_1^2 + x_2^2}$ and $\theta = \tan^{-1}(x_2/x_1)$. The condition $\gamma(\theta) + \gamma''(\theta) > 0$ to avoid ill-posedness is a standard assumption in interface motion [Gur93, Chapter 9]. The PDE (4) for smooth $\phi$ is still solvable numerically using conventional, explicit finite difference schemes. However, for non-smooth $\phi$ (and thus non-smooth $\gamma$) such as the crystalline case, the term $\gamma + \gamma''$ causes obvious impracticability.

Another approach to mean curvature motion is to solve a sequence of variational minimizations, originally introduced in [ATW93]. The formulation is as follows: let $h(C)$ be a small deformation of a closed curve $C$, and $\delta\mathcal{E}_\phi$ and $v$ be the first variation and gradient of $\mathcal{E}_\phi$, respectively. Then, for a small 'time-step' $\Delta t$, find the deformation $h^*$ that minimizes

$$\mathcal{E}_\phi(h(C)) - \mathcal{E}_\phi(C) + \frac{1}{2\Delta t}\langle h, h\rangle. \tag{5}$$

The claim is that, $h^*$ is an approximation to the evolution of $C$ by time $\Delta t$. This process is repeated iteratively to form a sequence of approximations to the evolution of $C$ under mean curvature flow. Intuitively, this comes from observing that $\mathcal{E}_\phi(h(C)) - \mathcal{E}_\phi(C) \approx \delta\mathcal{E}_\phi(C) = \langle v, h\rangle$ and that the minimizer of

$$\langle v, h\rangle + \frac{1}{2\Delta t}\langle h, h\rangle \tag{6}$$

is exactly $h = -v\Delta t$, the gradient flow of $\mathcal{E}_\phi$. Later, Chambolle [Cha04] showed that minimizing (5) can be achieved by defining $u : \Omega \subset \mathbb{R}^2 \to \mathbb{R}$ such that $C = \{x \in \Omega : u(x) = 0\}$ and considering the minimization

$$\min_{w \in L^2(\Omega)} \int_\Omega \phi(\nabla w) + \frac{1}{2\Delta t}||w - d(u)||_2 \tag{7}$$

where $d(u)$ is the signed distance function to $\{u \leq 0\}$, and $||\cdot||_2$ is the usual $L^2$ norm. The first term is the anisotropic total variation, see the definition (9) below. If $w^*$ is the minimizer of (7), then $h^*(C) = \{x \in \Omega : w^*(x) = 0\}$. In the case $\phi = |\cdot|$, (7) is the Rudin-Osher-Fatemi (ROF) functional used for image denoising [ROF92]. From a numerical standpoint, this approach to mean curvature flow has gained attention recently due to the advent of fast ROF solvers combined with well-known efficient methods for computing the distance function. See for example, [Cha04, GBO09].

The Split Bregman method, proposed by Goldstein and Osher [GO09] is a general and efficient technique for $L_1$ regularized minimization problems. The application of this method to solve the isotropic mean curvature problem via (7) was subsequently presented in [GBO09]. There, the authors briefly note that the generalization to the anisotropic case rests on the *anisotropic shrinkage problem*:

$$\text{given } x \in \mathbb{R}^2, \text{ find } \arg\min_{y \in \mathbb{R}^2} \phi(y) + \frac{1}{2}|x - y|^2. \tag{8}$$

The solution to this problem is given by

$$y = x - \pi_{\mathcal{W}_\phi}(x)$$

where $\pi_{\mathcal{W}_\phi}(z)$ is the projection of $z$ onto $\mathcal{W}_\phi$, the Wulff shape of $\phi$, see (13).

The first contribution of this article is to present a solution to (8) for a polyhedral norm $\phi$; this correspondingly solves the crystalline mean curvature problem. We will present the relevant details behind the Split Bregman method in Section 2.2.

The second contribution for anisotropic mean curvature flow is also based on (7) and the Split Bregman method, but follows a very different approach to the first. Inspired by [OBG+05], we construct an *inverse scale space flow*, a system of nonlinear ODE's where $u$ converges continuously to $w^*$. We formulate such a flow for smooth $\phi$.

## 2. The Split Bregman method

We first lay out a known algorithm for isotropic mean curvature flow, as presented in [GBO09]. This will be the prototype for the anisotropic mean curvature flow algorithms described later.

2.1. **Definitions and notations.** Throughout this article, $\Omega$ will be a bounded, connected, open subset in $\mathbb{R}^2$. Define the *total variation* of a function $u \in L^1_{loc}(\Omega)$ to be

$$\int_\Omega |\nabla u| := \sup\left\{ \int_\Omega u(x) \mathrm{div}\, \psi(x) dx : \psi \in C_0^1(\Omega), |\psi(x)| \leq 1, \forall x \in \Omega \right\}. \tag{9}$$

The space of all functions $u \in L^1(\Omega)$ such that $\int_\Omega |\nabla u| \leq \infty$ is the set $BV(\Omega)$, for which $\int_\Omega |\nabla u|$ becomes a semi-norm. Likewise, for a given positively 1-homogeneous function $\phi$, we can define the *anisotropic total variation* [EO04] as

$$\int_\Omega \phi(\nabla u) := \sup\left\{ \int_\Omega u(x) \mathrm{div}\, \psi(x) dx : \psi \in C_0^1(\Omega), \phi^\circ(\psi(x)) \leq 1, \forall x \in \Omega \right\}, \tag{10}$$

where $\phi^\circ$ is the *dual norm* (or *polar*) of $\phi$:

$$\phi^\circ(x) := \sup_{\phi(y) \leq 1} x \cdot y. \tag{11}$$

The unit ball of the energy function is known as the *Frank diagram*:

$$\mathcal{F}_\phi := \{y \in \mathbb{R}^2 \mid \phi(y) \leq 1\}. \tag{12}$$

The *Wulff shape* of $\phi$ is the unit ball of its dual norm:

$$\mathcal{W}_\phi := \left\{ y \in \mathbb{R}^2 : \phi^\circ(y) \leq 1 \right\}, \tag{13}$$

and in fact, by duality

$$\phi(x) = \sup_{y \in \mathcal{W}_\phi} y \cdot x;$$

(See Appendix A for formulae of dual norms for special cases.) this is precisely the definition of a dual norm [BV04, Appendix A].

*Examples.* A standard example of a dual pair of crystalline norms is the 1-norm $\|\cdot\|_1$ and the max-norm $\|\cdot\|_\infty$. For $p > 1$, the dual norm of a $p$-norm $\|\cdot\|_p$ is the $q$-norm with $1/p + 1/q = 1$. For a positive definite invertible matrix $A$, the norm $\phi(x) = \|Ax\|$ has the dual $\phi(x) = \|A^{-1}x\|$.

The *signed distance function* to a set $S \subset \Omega$ is $d_S(x) := dist(x, S) - dist(x, \Omega \backslash S)$. We will frequently make use of the signed distance function to a zero level set of another function $u$:

$$d(u)(x) := d_{\{u \leq 0\}}(x). \tag{14}$$

2.2. **The Split Bregman Method.** We briefly describe the Split Bregman method applied to the ROF functional. For further details we refer the reader to [GO09].

Let $\Omega \subset \mathbb{R}^2$ be a bounded, connected set, $f \in BV(\Omega)$, and $\lambda > 0$ be a real parameter. We seek to minimize the ROF functional

$$\int_\Omega |\nabla u| + \frac{\lambda}{2} ||u - f||_2^2 \tag{15}$$

over the set of all $u \in L^2(\Omega)$. The key idea is to consider the following constrained minimization problem:

$$\min_{u,d} J(u, d) = ||d||_1 + \frac{\lambda}{2} ||u - f||_2^2 \quad \text{such that} \quad d = \nabla u. \tag{16}$$

Then, (16) is solved by the *Bregman iteration* [Brè67, OBG+05]:

$$(u^{k+1}, d^{k+1}) = \arg\min_{u,d} D_J^{p_u^k, p_d^k}(u, u^k, d, d^k) + \frac{\mu}{2}||d - \nabla u||_2^2 \tag{17}$$

$$p_u^{k+1} := \partial_u J(u^k, d^k) = \mu(u^k - f) \tag{18}$$

$$p_d^{k+1} := \partial_d J(u^k, d^k) = \partial_d ||d^k||_1 \tag{19}$$

where $\partial_u J(u,k)$ and $\partial_d J(u,k)$ denote the $u$ and $d$ subgradients of $J(u,k)$, respectively, and $D_J^{p_u^k, p_d^k}(u, u^k, d, d^k)$ is the *Bregman distance*[Brè67] of $J(\cdot,\cdot)$:

$$D_J^{p_u^k, p_d^k}(u, u^k, d, d^k) := J(u,d) + J(u^k, d^k) - \langle p_u^k, u - u^k\rangle - \langle p_d^k, d - d^k\rangle. \tag{20}$$

The initial condition is set to $u^0 = f, d^0 = p_u^0 = p_d^0 = 0$. Then under suitable conditions, $u^k$ converges to the minimizer of (15). It can be shown that the iterative sequence (17), (18) and (19) can be equivalently written as,

$$(u^{k+1}, d^{k+1}) = \arg\min_{u,d} ||d||_1 + \frac{\lambda}{2}||u - f||_2^2 + \frac{\mu}{2}||d - \nabla u - b^k||_2^2 \tag{21}$$

$$b^{k+1} = b^k + (\nabla u^k - d^{k+1}), \tag{22}$$

where $b^0 = 0$. The iterative method (21) and (22) is called the *Split Bregman algorithm* for the ROF functional (15). To find the minimizer of (21), the authors in [GO09] use a two-step alternating minimization:

$$u^{k+1} = \arg\min_{u} \frac{\lambda}{2}||u - f||_2^2 + \frac{\mu}{2}||d^k - \nabla u - b^k||_2^2 \tag{23}$$

$$d^{k+1} = \arg\min_{d} ||d||_1 + \frac{\mu}{2}||d - \nabla u^{k+1} - b^k||_2^2. \tag{24}$$

The first can be solved via direct calculus; taking the gradient of the argument and setting it to zero yields an elliptic PDE for the minimizer $u^{k+1}$:

$$(\lambda - \mu\Delta)u^{k+1} = \lambda f - \mu\nabla\cdot(d^k - b^k). \tag{25}$$

For the second minimization, for numerical implementation purposes, we consider its discrete analogue: given vectors $\nabla u^{k+1}$, $b^{k+1} \in \mathbb{R}^2$, find $d^{k+1} \in \mathbb{R}^2$ such that

$$d^{k+1} = \arg\min_{d\in\mathbb{R}^2} |d| + \frac{\mu}{2}|d - \nabla u^{k+1} - b^k|^2. \tag{26}$$

This is known as a *shrinkage* (or *soft thresholding*) *problem*; the minimizer has a remarkably simple formula:

$$d^{k+1} = \text{shrink}(\nabla u^k - b^k, 1/\mu) := \max(|\nabla u^k - b^k| - 1/\mu, 0)\frac{\nabla u^k - b^k}{|\nabla u^k - b^k|}. \tag{27}$$

Later, in Section 3.1, we will consider the shrinkage problem from a more general perspective.

2.3. **Isotropic mean curvature flow.** We now apply the Split Bregman algorithm to Chambolle's formulation for isotropic mean curvature flow.

Consider an initial closed contour $C^0 = \partial S^0$, where $S^0$ is an open subset in $\Omega$. The goal is to approximate $C(t)$, the mean curvature flow of $C(0) = C^0$, for $t > 0$. For a fixed $\Delta t > 0$, let $w_{S^0}^* \in L^2(\Omega)$ be the minimizer of the ROF functional (15) with $\lambda = 1/(2\Delta t)$ and $f = d_{S^0}$. Define the operator $T_{\Delta t}(S^0) := \{x \in \Omega : w_{S^0}^*(x) < 0\}$. Then, for $t > 0$, let

$$S_{\Delta t}(t) = (T_{\Delta t})^{[t/\Delta t]}(S^0). \tag{28}$$

It is proved in [Cha04] that $C_{\Delta t}(t) = \partial S_{\Delta t}(t)$ for $t > 0$ is the discrete time approximation to the mean curvature flow of the initial contour $C^0$. Furthermore, (28) implements a *monotone* curve evolution of the flow introduced by Almgren, Taylor and Wang [ATW93]; that is, $S \subset S'$ implies $T_{\Delta t}(S) \subset T_{\Delta t}(S')$.

For the actual implementation, it is more convenient to work with level set functions rather than sets. Let $u_j(x) := d_{(T_{\Delta t})^j(S^0)}(x), j = 0, 1, 2...$, the sequence of distance functions to the sets $S^j := (T_{\Delta t})^j(S^0), j = 0, 1, 2....$ Clearly, the zero level sets of $u_j(x)$ form the discrete time approximation of the evolution of $S^0$.

We outline the Split Bregman approach to isotropic mean curvature flow in Algorithm 1. The inner loop in $k$ corresponds to the Split Bregman iteration for the ROF functional. The outer loop in $j$ corresponds to the discrete time iteration of the approximation: $C(j\Delta t) \approx C_{\Delta t}(j\Delta t) = \{u_j(x) = 0\}$.

**Input**: $u_0 = d_{S^0}$, final time $T > 0$, parameter $\mu > 0$.
**Output**: $u_{[T/\Delta t]} = d_{S_{\Delta t}(t)}$.
**foreach** $j = 0, 1, ..., [T/\Delta t]$ **do**
  Set $f \leftarrow u_j$;
  Initialize $u_j^0 \leftarrow u_j, b^0 = d^0 = 0$;
  **foreach** $m = 0, 1, ..., N$ **do**
    Solve $\left(\frac{1}{2\Delta t} - \mu\Delta\right) u_j^{m+1} = \frac{1}{2\Delta t} f - \mu\nabla \cdot (d^m - b^m) \rightarrow u_j^{m+1}$;
    $d^{m+1} \leftarrow \text{shrink}(\nabla u_j^m - b^m, 1/\mu)$;
  **end**
  $u_{j+1} \leftarrow d(u_j^N)$;
**end**

**Algorithm 1**: Isotropic mean curvature flow using the Split Bregman algorithm.

## 3. Crystalline Mean Curvature Flow

3.1. **Polyhedral shrinkage.** In this section we show that the generalized shrinkage problem is equivalent to the projection onto the Wulff shape. Thus we can obtain explicit solutions for the generalized shrinkage problem for a *polyhedral norm*.

Start by writing $\phi$ as

$$\phi(x) = \sup_{z \in \mathcal{W}_\phi} z \cdot x, \tag{29}$$

and define $\pi_{\mathcal{W}_\phi}(z)$ to be the projection of $z$ onto $\mathcal{W}_\phi$,

$$\pi_{\mathcal{W}_\phi}(y) = \arg\min_{x \in \mathcal{W}_\phi} |x - y|^2.$$

Consider the quadratic plus norm minimization problem

$$x^* = x^*(y) = \arg\min_{x \in \mathbb{R}^n} \left\{ \phi(x) + \frac{1}{2}|x - y|^2 \right\}. \tag{30}$$

Then we claim the following characterization holds.

*Lemma* 1.

$$x^*(y) = y - \pi_{\mathcal{W}_\phi}(y). \tag{31}$$

*Proof.* Rewrite the minimization in (30) using (29) as

$$\min_{x\in\mathbb{R}^n}\max_{z\in\mathcal{W}_\phi}\left\{\frac{1}{2}|x-y|^2+z\cdot x\right\}.$$

Since the inner function is convex in $x$ and affine in $y$, we can interchange the order of min and max to obtain

$$\max_{z\in\mathcal{W}_\phi}\min_{x\in\mathbb{R}^n}\left\{\frac{1}{2}|x-y|^2+z\cdot x\right\}.$$

Evaluate the inner problem to obtain

$$x=y-z,$$

which results in $\max_{z\in\mathcal{W}_\phi}\left\{-\frac{1}{2}z^2+z\cdot y\right\}$, or equivalently,

$$\min_{y\in\mathcal{W}_\phi}\left\{\frac{1}{2}|z-y|^2\right\}.$$

The last problem is a projection problem, giving

$$z=\pi_{\mathcal{W}_\phi}(y).$$

The last result, together with $x=y-z$, yields (31). □

Using the last lemma, we can characterize $y$ in (30) such that the minimizer $x^*(y)$ is zero.

*Proposition* 1. $y\in\mathcal{W}_\phi$ if and only if $x^*(y)=0$.

*Proof.* This is an immediate consequence of (31). □

In this section, from hereon, we let $\phi$ be a polyhedral norm. Given a set of normals $\mathcal{N}=\{n_i\}_{i=1}^k\subset\mathbb{R}^2$ ordered clockwise (define $n_{n+1}=n_1$ and $n_0=n_k$), write

$$\phi(x)=\max_{n_i\in\mathcal{N}} n_i\cdot x. \tag{32}$$

Partition $\mathbb{R}^2\backslash\{0\}$ into the regions:

$$\begin{aligned} C_i &= \{x\neq 0 : n_i\cdot x > n_j\cdot x \text{ for } j=1,...,k\} \qquad i=1,...,k\\ R_{i,i+1} &= \{x\neq 0 : n_i\cdot x = n_{i+1}\cdot x > 0\} \qquad i=1,...,k \end{aligned}$$

Thus, $\phi$ is smooth in $C_i$ and has a kink along the rays $R_{i,i+1}$. With Proposition 1, we are left with characterizing the minimizer for the case $y\notin\mathcal{W}_\phi$ (equivalently $\phi^\circ(y)>1$).

**Theorem 1** (Polyhedral Shrinkage Formula)**.** *Assume that the normals in* (32) *are ordered clockwise, and that $\phi^\circ(y)>1$. Define, for each $i\in\{1,2,...,k\}$,*

$$\lambda_i=\lambda_i(y):=\frac{(n_i-n_{i+1})\cdot y+\|n_{i+1}\|^2-n_i\cdot n_{i+1}}{\|n_i-n_{i+1}\|^2}. \tag{33}$$

*Then, either $\lambda_i\in[0,1]$ or $\lambda_i>1$ and $\lambda_{i-1}<0$, for some unique $i$. Furthermore, in the former case,*

$$x^*(y)=y-(n_i\lambda_i+n_{i+1}(1-\lambda_i)), \tag{34}$$

*and for the latter case,*

$$x^*(y)=y-n_i. \tag{35}$$

*Proof.* Start by taking the subdifferential of (30),

$$0 \in \partial\phi(x^*) + (x^* - y). \tag{36}$$

The subdifferential $\partial\phi$ can be explicitly solved:

$$\partial\phi(x) = \begin{cases} n_i & : \quad x \in C_i \\ \mathbf{conv}\{n_i, n_{i+1}\} & : \quad x \in R_{i,i+1} \end{cases} \tag{37}$$

In light of Proposition 1, $y \notin \mathcal{W}_\phi$ implies that $x^*(y) \in \mathbb{R}^2/\{0\}$. Since $\{C_i, R_{i,i+1}\}_{i=1}^k$ partitions $\mathbb{R}^2/\{0\}$, it will be sufficient to consider the cases $x^*(y) \in C_i$ or $x^*(y) \in R_{i,i+1}$, for some $i$.

Rearrange (36) and consider the case when $x^* \in R_{i,i+1}$ for some $i$. Clearly, we have

$$y - (n_i\lambda + n_{i+1}(1-\lambda)) = x^* \tag{38}$$

for some unique $\lambda \in [0,1]$. Muliplying (38) by $n_i$ and $n_{i+1}$, and noting that $n_i \cdot x^* = n_{i+1} \cdot x^*$, one can solve for $\lambda$: the solution is $\lambda = \lambda_i$ as per (33). Setting $\lambda = \lambda_i$ in (38) gives (34).

For the case $x^* \in C_i$, we have

$$y - n_i = x^*. \tag{39}$$

To see that $\lambda_i > 1$ and $\lambda_{i-1} < 0$ in this case, note that if $x^* \in C_i$,

$$x^* \cdot n_i > x^* \cdot n_j, \quad \forall j \neq i. \tag{40}$$

Therefore, since $y = x^* + n_i$,

$$\begin{aligned} \lambda_i(y) &= \frac{(n_i - n_{i+1}) \cdot x^*}{\|n_i - n_{i+1}\|^2} + 1 > 1 \\ \lambda_{i-1}(y) &= \frac{(n_{i-1} - n_i) \cdot x^*}{\|n_i - n_{i+1}\|^2} < 0. \end{aligned}$$

□

Theorem 1 can be immediately restated as an algorithm, see Algorithm 2.

**Input**: Normals $\{n_i\}_{i=1}^k$ as per (32), $y \in \mathbb{R}^2$.
**Output**: Solution to the shrinkage problem $x^*$ in (31).
**foreach** $i = 1, ..., k$ **do**
  Compute $\lambda_i(y)$ (see (33));
  **if** $\lambda_i \in [0,1]$ **then**
    $x^* \leftarrow y - (n_i\lambda_i + n_{i+1}(1-\lambda_i))$
  **end**
  **if** $\lambda_i > 1$ *and* $\lambda_{i+1} < 0$ **then**
    $x^* \leftarrow y - n_i$
  **end**
**end**

**Algorithm 2**: Polyhedral shrinkage algorithm.

We illustrate the result of the Proposition 1 in Figure 3.1, by computing shrinkage for the octagon norm $\phi_8$, where the eight normals are

$$\{(\pm 1, 0), (0, \pm 1), (\pm 1, \pm 1)/\sqrt{2}, (\pm 1, \mp 1)/\sqrt{2}\}. \tag{41}$$

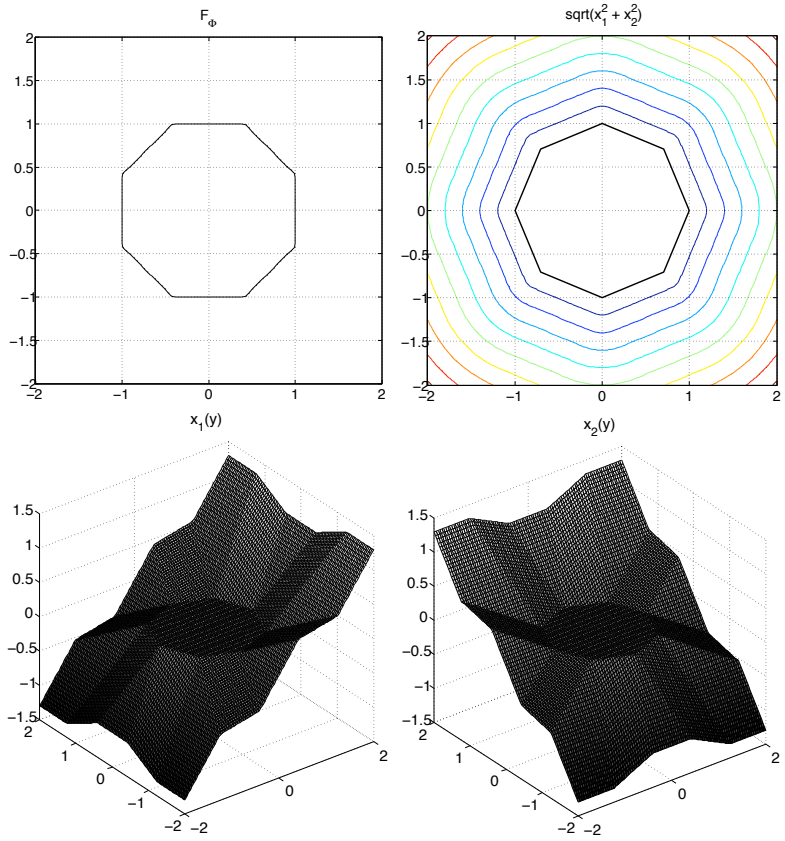


Figure 1: Top left: the Frank diagram for the octagon $\phi_8$. Top right: contour plot of $|x^*(y)|$. The dark contour is the zero level set; note that this is the Wulff shape for $\phi_8$. Bottom left and right: a surface plot of the components of $x^*(y) = (x_1(y), x_2(y))$.

3.2. **Algorithm for the crystalline case.** The polyhedral shrinkage algorithm (Algorithm 2) provides the key ingredient to modify Algorithm 1 for crystalline energies. We omit presenting the complete algorithm for the crystalline case since it only differs from Algorithm 1 at a single line; namely, the line $d^{m+1} \leftarrow \text{shrink}(\nabla u_j^m - b^m, 1/\mu)$ should be replaced by Algorithm 2 with inputs $y = \nabla u_j^m - b^m$ and the set of normals $\{n_i\}_{i=1}^k$ corresponding to the Frank diagram, scaled accordingly by $\mu$.

*Remark.* As pointed out in [Cha04], the necessary modification for solving (3) to Algorithm 1 is the last line, which should be replaced by:

$$u_{j+1} \leftarrow d^{\phi^\circ}(u_j^N),$$

where $d^{\phi^\circ}(u)$ is the distance in the $\phi^\circ$ metric to the zero level set of $u$.

The complexity for Algorithm 2 is clearly $O(k)$, where $k$ is the number of normals representing the energy in (32). Thus, the computational cost for evolving a

crystalline mean curvature flow is $O(k)$ times that of the isotropic mean curvature flow (Algorithm 1).

## 4. Smooth Anisotropic Mean Curvature Flow

4.1. **Motivation.** We saw in the last section that an explicit characterization of shrinkage was possible for a polyhedral anisotropy on $\phi$. However, for a smooth anisotropic $\phi$, such characterization of shrinkage seems to be difficult, in general. As a quick illustration, consider the norm

$$\phi(x) = \sqrt{2x_1^2 + x_2^2} \quad x = (x_1, x_2). \tag{42}$$

Then, its dual norm $\phi^\circ(x) = \sqrt{\frac{1}{2}x_1^2 + x_2^2}$, has a unit ball of an ellipse elongated in the $x_2$ direction. Thus, shrinkage for $\phi$ amounts to computing the closest point to this ellipse. A calculus argument shows that such a task requires one to solve a non-trivial quartic equation. One may easily see that deriving a shrinkage formula a more complicated smooth norm becomes quickly difficult.

4.2. **Inverse Scale Space formulation.** Alternatively, we derive an inverse scale space flow [OBG+05] arising from the Split Bregman method for (17). Throughout this section, we write the norm $\phi$ as follows:

$$\phi(x) = \gamma(\theta)\|x\|, \quad \theta = \tan^{-1}(x_2/x_1), \tag{43}$$

and assume that $\gamma$ is a smooth, 0-homogeneous, $2\pi$-periodic function.

Consider the Bregman iterative update formulae (17), (18) and (19) for the Split Bregman minimization problem (16). For clarity, we write out the right hand side of (18) using the definition of the Bregman distance with $h = \Delta t$ (this is to avoid subsequent ambiguity with the Laplacian operator):

$$\min_{d,u} \int \gamma(\theta)|d| + \frac{1}{2h}\int |u-f|^2 - \langle p_u^k, u - u^k\rangle - \langle p_d^k, d - d^k\rangle + \frac{\lambda}{2}\int |d - \nabla u|^2, \tag{44}$$

where $\theta = \tan^{-1}(d_2/d_1)$. First, taking the Euler-Lagrange derivative of the functional with respect to $d$ gives,

$$p_d^{k+1} - p_d^k + \lambda(d^k - \nabla u^k) = 0. \tag{45}$$

Observing (45) as a forward Euler update scheme over a time variable $s$ with step size $\lambda$, it approximates the PDE

$$\frac{\partial p_d}{\partial s} = \nabla u - d. \tag{46}$$

For brevity, let us denote $d = Rp$, for $R$ scalar and $p = (\cos\theta, \sin\theta)$ a unit vector. By the smoothness assumption of $\gamma$,

$$\begin{aligned} p_d = \partial_d \int |d|\gamma(\theta) &= \frac{d}{|d|}\gamma(\theta) + |d|\gamma'(\theta)\nabla_d\theta(d) \\ &= \frac{d}{|d|}\gamma(\theta) + \frac{d^\perp}{|d|}\gamma'(\theta) \quad \text{where } d^\perp = (-d_2, d_1) \\ &= p\gamma(\theta) + p^\perp\gamma'(\theta) \quad \text{where } p^\perp = (-p_2, p_1), \end{aligned}$$

thus,

$$\begin{aligned}\frac{\partial p_d}{\partial s} &= (-\sin\theta,\cos\theta)\frac{\partial\theta}{\partial s}\gamma(\theta) + (\cos\theta,\sin\theta)\frac{\partial\theta}{\partial s}\gamma'(\theta) \\ &\quad -(\cos\theta,\sin\theta)\frac{\partial\theta}{\partial s}\gamma'(\theta) + (-\sin\theta,\cos\theta)\frac{\partial\theta}{\partial s}\gamma''(\theta) \\ &= p^\perp(\gamma(\theta)+\gamma''(\theta))\frac{\partial\theta}{\partial s}.\end{aligned}$$

Substituting the latter result into (46),

$$p^\perp(\gamma+\gamma'')\frac{\partial\theta}{\partial s} = \nabla u - Rp. \tag{47}$$

If we multiply (47) by $p$,

$$\begin{aligned}0 &= p\cdot\nabla u - R|p|^2 \\ R &= p\cdot\nabla u,\end{aligned}$$

and if we multiply (47) by $p^\perp$,

$$\begin{aligned}(\gamma+\gamma'')\frac{\partial\theta}{\partial s} &= p^\perp\cdot\nabla u - Rp^\perp\cdot p \\ \frac{\partial\theta}{\partial s} &= \frac{p^\perp\cdot\nabla u}{\gamma+\gamma''}.\end{aligned}$$

Next taking the derivative of the functional in (44) with respect to $u$,

$$p_u^{k+1} - p_u^k - \lambda(\nabla\cdot d - \Delta u^k) = 0. \tag{48}$$

Since the $u$ subgradient is explicitly $p_u = \frac{1}{h}(u-f)$,

$$\frac{1}{h}(u^{k+1}-f) - \frac{1}{h}(u^k - f) - \lambda(\nabla\cdot d - \Delta u^k) = 0, \tag{49}$$

and again taking $\lambda$ to be the step size of a forward Euler discretization, the PDE for $u$ becomes

$$\frac{\partial u}{\partial s} = h(\Delta u - \nabla\cdot d). \tag{50}$$

To summarize, the system of PDE's describing the inverse scale space flow of (17) with smooth anisotropy is,

$$\frac{\partial\theta}{\partial s} = \frac{p^\perp\cdot\nabla u}{\gamma+\gamma''}, \tag{51}$$

$$\frac{\partial u}{\partial s} = h(\Delta u - \nabla\cdot d), \tag{52}$$

where

$$R = p\cdot\nabla u, \qquad d = Rp. \tag{53}$$

To describe the initial condition, we abuse notation and write $u, d, R, \theta, p, p_u, p_d$ solely as functions of $s$; e.g. $u(x_1,x_2,s) = u(s)$. Following [BGOX06], the initial conditions for an inverse scale space flow are $d(0)=0$, $p_d(0)=0$, $p_u(0)=0$. Immediately, we have $R(0) = |d(0)| = 0$. Since $0 = p_u(0) = (u(0)-f)$, we also have $u(0) = f$. Consequently, since $0 = R(0) = p(0)\cdot\nabla u(0) = p(0)\cdot\nabla f$ holds, $p(0) = (-f_y, f_x) \equiv \nabla^\perp f$, and therefore, $\theta(0) = \tan^{-1}(-f_x, f_y)$. In conclusion,

$$u(0) = f, \quad p(0) = \nabla^\perp f, \quad \theta(0) = \tan^{-1}(-f_x/f_y), \quad R(0) = 0. \tag{54}$$

*Remark.* The appearance of the Laplacian operator in (52) bears resemblence to the MBO scheme for mean curvature flow [MBO94]. The MBO scheme solves the mean curvature flow by repeating: 1. evolve the heat equation for a short time, and 2. thresholding. A precise connection between the two schemes is a subject of future investigation.

4.3. **Properties of the inverse scale space flow.** The following proposition lists several immediate consequences from the inverse scale flow.

*Proposition* 2. Suppose $u$, $d$, $R$, $p$, $\gamma$ and $\theta$ satisfies (51)-(53). Then,

1. $u = h(\gamma + \gamma'')\nabla \cdot p + f$.
2. $\frac{\partial}{\partial s}\|u\|^2 \leq 0$ (decrease in energy).
3. If $R(s) \geq 0$ then $\frac{\partial}{\partial s}\|\nabla u - d\| \leq 0$.
4. $\frac{\partial \theta}{\partial s}(s) > 0$ for $s \geq 0$ until steady state.

*Proof.* 1. One can verify directly: $\nabla \cdot p_d = \nabla \cdot (p\gamma + p^\perp \gamma) = (\gamma + \gamma'')\nabla \cdot p$. By (52) and the latter result,

$$\frac{\partial u}{\partial s} = h\nabla \cdot (\nabla u - d) = h\nabla \cdot \frac{\partial p_d}{\partial t} = h\frac{\partial}{\partial s}(\gamma + \gamma'')\nabla \cdot p. \tag{55}$$

Integrating over $s$, and considering the initial conditions $u(0) = f, p(0) = \nabla^\perp f$, one arrives at the desired result.

2. By direct differentiation,

$$\begin{aligned}
\frac{1}{2}\frac{\partial}{\partial s}\|u\|^2 &= \int u\frac{\partial u}{\partial s}dx \\
&= h\int u(\Delta u - \nabla \cdot d) \\
&= h\left(-\int |\nabla u|^2 + \int \nabla u \cdot d\right) \\
&= h\left(-\|\nabla u\|^2 + \|R\|^2\right) \\
&\leq 0.
\end{aligned}$$

The last inequality holds since by (53), $|R| = |p \cdot \nabla u| \leq |\nabla u|$.

3. Assume $\gamma + \gamma'' > 0$ for well-posedness and by assumption $R(s) \geq 0$. Then we can define a seminorm

$$\|\cdot\|_{(\gamma+\gamma'')R} := \left[\langle(\gamma + \gamma'')R(s)\cdot, \cdot\rangle\right]^{\frac{1}{2}}. \tag{56}$$

Since,

$$\frac{\partial d}{\partial s} = \frac{\partial R}{\partial s}p + R\frac{\partial p}{\partial s} = \frac{\partial R}{\partial s}p(t) + p^\perp\frac{\partial \theta}{\partial s}, \tag{57}$$

we have

$$\begin{aligned}
\frac{\partial}{\partial s}\frac{1}{2}\|\nabla u - d\|^2 &= \langle \nabla u - d, \frac{\partial}{\partial s}(\nabla u - d)\rangle \\
&= -\langle \Delta u - \nabla\cdot d, \frac{\partial u}{\partial s}\rangle - \langle \nabla u - d, \frac{\partial R}{\partial s}p(t) + Rp^\perp \frac{\partial \theta}{\partial s}\rangle \\
&= -\frac{1}{h}\left\|\frac{\partial u}{\partial s}\right\|^2 - \langle p\cdot(\nabla u - d), \frac{\partial R}{\partial s}\rangle - \langle p^\perp\cdot(\nabla u - d), R\frac{\partial \theta}{\partial s}\rangle \\
&= -\frac{1}{h}\left\|\frac{\partial u}{\partial s}\right\|^2 - \langle R - R, \frac{\partial R}{\partial s}\rangle - \langle (\gamma+\gamma'')\frac{\partial \theta}{\partial s}, R\frac{\partial \theta}{\partial ts}\rangle \\
&= -\frac{1}{h}\left\|\frac{\partial u}{\partial s}\right\|^2 - \left\|\frac{\partial \theta}{\partial s}\right\|^2_{(\gamma+\gamma'')R} \\
&\le 0.
\end{aligned}$$

4. Clearly, $\frac{\partial\theta}{\partial s}(0) = |\nabla^\perp f|^2/(\gamma+\gamma'') > 0$. Consider the first instance $s = T$ for which $\frac{\partial\theta}{\partial s}(T) = 0$. Then by (51), $p(T)\cdot\nabla^\perp u(T) = 0$, thus $p(T) = \pm\nabla u(T)/|\nabla u(T)|$. Furthermore, by (53), $R(T) = \pm|\nabla u|$. Therefore, $d(T) = \nabla u(T)$, and so $\frac{\partial u}{\partial s}(T) = h\nabla\cdot(d(T) - \nabla u(T)) = 0$, so the flow has reached a steady state at $s = T$.

□

Result 4 of Proposition 2 shows that $d(s)$ turns counter-clockwise as $s$ increases. Note that initially, $d(0)$ is perpendicular to $\nabla u(0) = \nabla f$. Thus, $d(t)$ turns counter-clockwise until it coincides with $\nabla u$, at which point $\frac{\partial\theta}{\partial s} = 0$ and steady state is reached.

To better understand how the functions relate in the limit $s\to\infty$, we apply the results of the last proposition:

*Proposition* 3. Suppose $u$, $d$ and $\theta$ have sufficiently smooth limits as $s\to\infty$, namely $u_\infty$, $d_\infty$, $\theta_\infty$, respectively. Then

1. $\nabla u_\infty = d_\infty$.
2. $\frac{\partial}{\partial s}D(u_\infty, u(s), d_\infty, d(s)) \le 0$. (decay of Bregman distance)
3. Further assume that $|\nabla u_\infty| \neq 0$. Then

$$\frac{u_\infty - f}{h} = (\gamma(\theta_\infty) + \gamma''(\theta_\infty))\nabla\cdot\frac{\nabla u_\infty}{|\nabla u_\infty|}|\nabla f|. \tag{58}$$

*Proof.* 1. Suppose $\nabla u_\infty - d_\infty = v$, for some constant $v\in\mathbb{R}^2$. Then

$$\begin{aligned}
p_\infty\cdot v &= p_\infty\cdot\nabla u_\infty - p_\infty\cdot d_\infty \\
&= R_\infty - R_\infty = 0,
\end{aligned}$$

and

$$\begin{aligned}
p_\infty^\perp\cdot v &= p_\infty^\perp\cdot\nabla u_\infty - p_\infty^\perp\cdot d_\infty \\
&= (\gamma(\theta_\infty)+\gamma''(\theta_\infty))\frac{\partial\theta_\infty}{\partial s} - p^\perp\cdot R_\infty p_\infty \\
&= 0 - 0 = 0.
\end{aligned}$$

Therefore, $v = 0$.

2. By direct differentiation:

$$\begin{aligned}
\frac{\partial}{\partial s} D(u_\infty, u, d_\infty, d) &= \langle p_d, \frac{\partial d}{\partial s}\rangle + \langle \frac{u-f}{h}, \frac{\partial u}{\partial s}\rangle - \langle \frac{1}{h}\frac{\partial u}{\partial s}, u_\infty - u\rangle \\
&\quad -\langle \frac{u-f}{h}, \frac{\partial u}{\partial s}\rangle - \langle \frac{\partial p_d}{\partial s}, d_\infty - d\rangle - \langle p_d, \frac{\partial d}{\partial s}\rangle \\
&= -\langle \nabla\cdot(\nabla u - d), u_\infty - u\rangle - \langle \nabla u - d, d_\infty - d\rangle \\
&= \langle \nabla u - d, \nabla u_\infty - \nabla u - (d_\infty - d)\rangle \\
&= -\|\nabla u - d\|^2 \qquad \text{since } \nabla u_\infty = d_\infty \\
&\leq 0.
\end{aligned}$$

3. From the first result,

$$p_\infty = \frac{\nabla u_\infty}{|\nabla u_\infty|}. \tag{59}$$

Substituting the above into the first result of Proposition 2 and rearranging gives the desired result. Note that $|\nabla f| = 1$, as $f$ is a distance function.

□

The last result in Proposition 3 elucidates the connection between (51)-(53) and the level set equation for mean curvature flow (4). In other words, solving the inverse scale space equation to steady state is equivalent to a semi-implicit forward Euler scheme for the time dependent PDE (4). While explicit forward Euler schemes suffer time step restrictions $h = O(dx^2)$ (where $dx$ is the spacial discretization), the semi-implict nature of the inverse scale space flow suggests that it may be free from such restrictions.

The results of Proposition 3 hinges on the assumption that both $u$ and $d$ converge to steady state solutions. Whether this assumption is generally true, is still an open question, although all of our numerical tests confirmed the affirmative. Our final result gives another convergence proof provided that $R(s)$ stays positive in the limit. We have observed that $R(s)$ may be zero for some $s > 0$ in general but seems to stay positive for all $s > 0$ for sufficiently smooth convex $f$.

*Proposition* 4. Suppose there exists $s^* > 0$ such that

$$R(s) \geq R_0 > 0 \qquad \forall s > s^*. \tag{60}$$

Then, $\|\nabla u(s) - d(s)\| \to 0$ as $s \to 0$.

*Proof.* We may assume that there exists $B > 0$ such that,

$$B \geq \gamma + \gamma'' > 0.$$

By (47), we can write

$$\|\nabla u - d\|^2 = \left\| (\gamma + \gamma'')\frac{\partial \theta}{\partial s} \right\|^2.$$

From the proof of Proposition 3, the last equality, and (60), for $s > s^*$,

$$\begin{aligned}
\frac{\partial}{\partial s}\frac{1}{2}\|\nabla u - d\|^2 &\leq -\left\langle \frac{\partial \theta}{\partial s}, \frac{\partial \theta}{\partial s}(\gamma + \gamma'')R(s)\right\rangle \\
&\leq -\frac{R_0}{B}\left\langle \frac{\partial \theta}{\partial s}, \frac{\partial \theta}{\partial s}(\gamma + \gamma'')^2\right\rangle \\
&= -\frac{R_0}{B}\|\nabla u - d\|^2.
\end{aligned}$$

By Gronwall's inequality, $\|\nabla u(s) - d(s)\| \leq \|\nabla u(0) - d(0)\| e^{-\frac{2R_0}{B}s} = e^{-\frac{2R_0}{B}s}$, so taking $s \to 0$ we have our result. □

4.4. **Algorithm for the smooth anisotropy case.** Algorithm 3 outlines the algorithm for smooth anisotropic mean curvature flow using the inverse scale space flow (51)-(53).

*Remark.* The trivial modification to the inverse scale space method for the evolution PDE (3) is to let (51) be

$$\frac{\partial \theta}{\partial s} = \frac{p^\perp \cdot \nabla u}{\gamma(\gamma + \gamma'')},$$

and all the results in the previous section holds true.

**Input**: $u_0 = d_{S^0}$, final time $T > 0$, time step $\Delta t > 0$.
**Output**: $u_{[T/\Delta t]} = d_{S_h(t)}$.
**foreach** $j = 0, 1, ..., [T/\Delta t]$ **do**
  Set $f \leftarrow u_j$;
  Initialize $u(0) \leftarrow f$, $p(0) \leftarrow \nabla^\perp f, \theta(0) \leftarrow \tan^{-1}(-f_x/f_y)$, $R(0) \leftarrow 0$;
  Solve (51)-(53) with $h = \Delta t$, until steady state: $\lim_{t\to\infty} u(t) = u_\infty$;
  Set $u_{j+1} \leftarrow d(u_\infty)$;
**end**

**Algorithm 3**: Anisotropic mean curvature flow using the inverse scale space flow.

## 5. Numerical Results

5.1. **Crystalline case.** We numerically solved the anisotropic mean curvature flow using the polyhedral shrinkage algorithm (Algorithm 2) within Algorithm 1. The PDE (25) for $u^{k+1}$ was solved using a standard finite difference discretization, and the distance functions were computed using the Fast Marching Method.

The norms (32) considered were:

- 1-norm: $\mathcal{N}_1 = \{\pm(1,1), \pm(1,-1)\}$.
- Octagon-norm: $\mathcal{N}_8 = \{(\pm 1, 0), (0, \pm 1), (\pm 1, \pm 1)/\sqrt{2}, (\pm 1, \mp 1)/\sqrt{2}\}$.
- A skewed hexagon norm: $\mathcal{N}_{skew} = \{(\pm 1, 0), (0, \pm 1), \pm(1, 1))\}$.
- A triangle 'norm': $\mathcal{N}_{tri} = \{(\sqrt{2}, \sqrt{2}), (-1, 0), (0, -1)\}$.

Figure 2 shows the results for these anisotropies on a $100 \times 100$ grid with $\Delta t = 0.015$. The outer and inner iterations were computed until a consecutive approximations were bounded by 2e-5. Typically, it took less than 20 outer iterations, while the inner iteration ranged from 2 to 500. Notice the emergence of the Wulff shapes as the curves near extinction; see Appendix A for Wulff shapes of anisotropic norms. Note that $\mathcal{N}_{tri}$ does not induce a norm due to its asymmetry, but the algorithm computes its flow nonetheless.

5.2. **Inverse scale space algorithm case.** We first present a sequence of plots showing how the inverse scale space flow (51)-(53) behaves. For the isotropic case ($\gamma = 1$) with time step $\Delta t = h = 0.015$, Figure 3 shows $\nabla u$, $d$ and the contour $\{u = 0\}$ at various stages in the iterations over $s$, where $\Delta s = 0.001$. Note how $\theta$ (the direction of $d$) moves clockwise as proven in Proposition 2, part 4. The stopping condition was $\|u^{n+1} - u^n\|_\infty \leq$ 1e-5, where $u^n$ is the $n$-th iterate approximating $u$, for which the iteration halted after 3770 iterations. We have observed that the

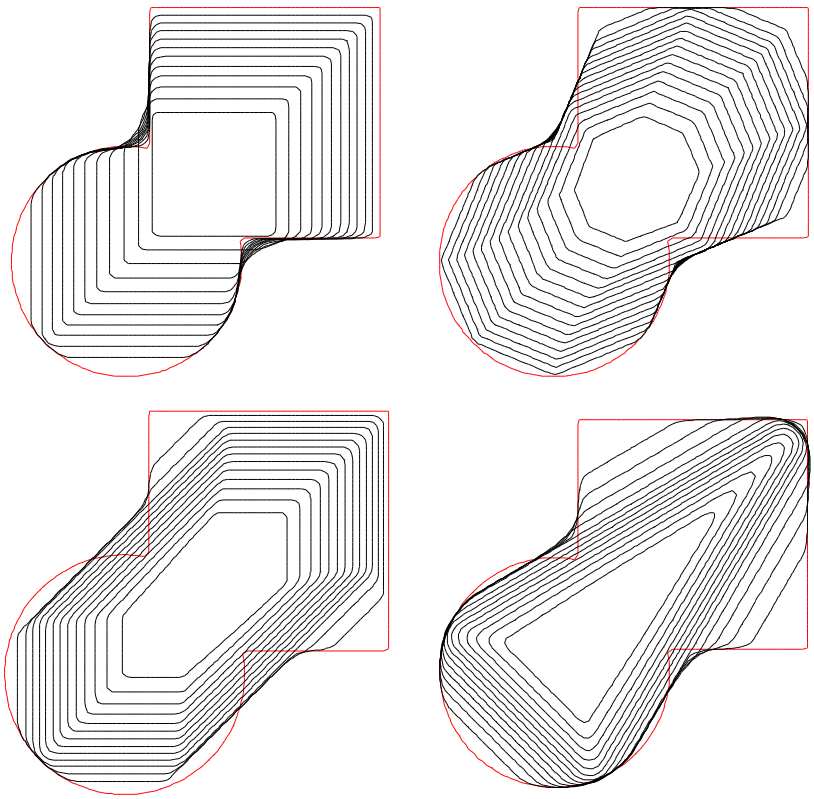

Figure 2: Crystalline mean curvature motion for various anisotropies. Clockwise from top left: $\mathcal{N}_1$, $\mathcal{N}_8$, $\mathcal{N}_{tri}$, and $\mathcal{N}_{skew}$

number of iterations necessary for convergence (for the same stopping condition and time step) was roughly between 3000 to 4000 for $N = 25, 50, 100, 150$. It is reasonable to believe that the number of iterations to convergence should remain constant for all $N$, since convergence is attained for a large enough $s$, which is problem dependent (choice of $\gamma$, $f$) and independent of the grid size.

Figure 5 shows the plot of $\|\nabla u - d\|$ over iterations in $s$ in (51)-(53), for various anisotropies. The anisotropies (43) tested were

$$\gamma_n(\theta) = \frac{1}{n^2+1}(n^2 + 1 - \sin(n\theta)), \quad \text{for } n = 0, 2, 4, 8. \tag{61}$$

Note that $n = 0$ is the isotropic case; for $n = 2, 4, 8$, the anisotropy has a $n$-fold rotational symmetry. We have found that, in general, the isotropic case converges faster to steady state than the anisotropic cases; also, for all cases tested, $\|\nabla u - d\|$ eventually converges exponentially, corroborating with the results of Proposition 4.

Results for Algorithm 3 are shown in Figure 4 for the anisotropies (61).

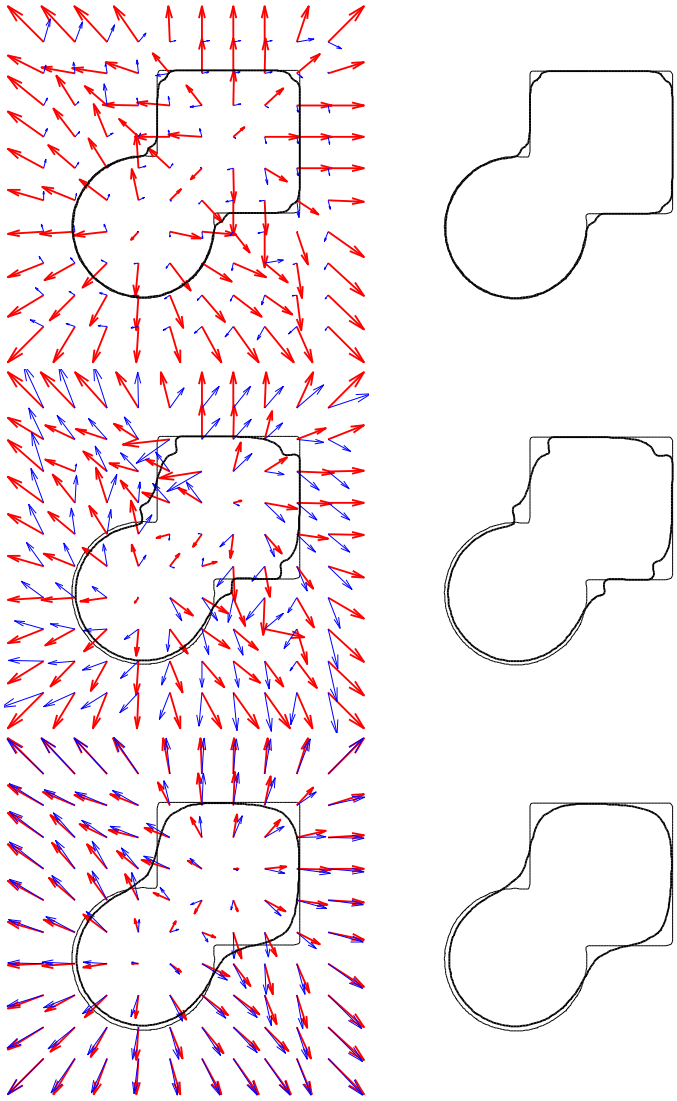

Figure 3: Visualization of $\nabla u$ and $d$ in the inverse scale space flow (51)-(53), with $\gamma_0 = 1$ (the isotropic case). Thick arrows are $\nabla u$ and the thin arrows are $d$. Top to bottom: 200, 1000, 3000 iterations.

## Acknowledgements

S. Osher and R. Takei were partially supported by ONR grants N00014-03-1-007, N00014-07-0810. R. Tsai was partially supported by NSF grant DMS-0714612.

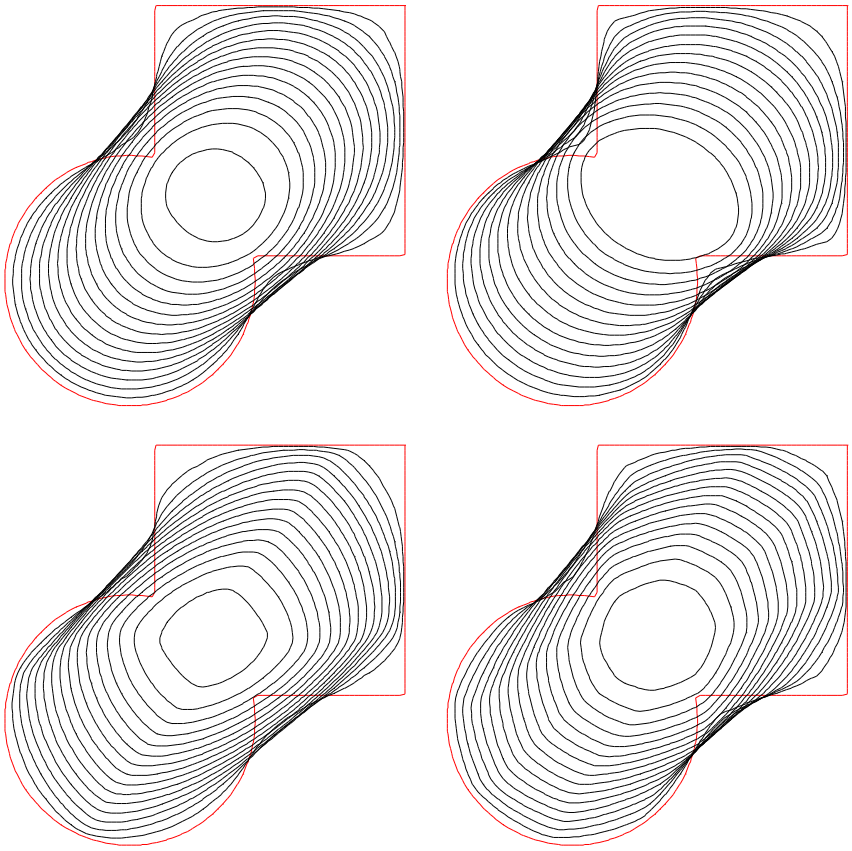

Figure 4: Mean curvature motion for various smooth anisotropies. Clockwise from top left: $\gamma_0$ (isotropic), $\gamma_2$, $\gamma_8$, and $\gamma_4$.

## Appendix A. Formulae for Wulff shapes

Define as per (32), a polyhedral norm as

$$\phi(x) = \max_{n_i \in \mathcal{N}} n_i \cdot x, \tag{62}$$

with dual norm $\phi^\circ$. We claim that the Wulff shape of $\phi$ is the polygon with vertices $\mathcal{N}$. To this end, we show that that $\phi^\circ(x) = 1$ on the polygon. Clearly,

$$\phi^\circ(n_i) = \max\{n_i \cdot y : \max_{n_j \in \mathcal{N}} \{n_j \cdot y\} = 1\} \leq 1. \tag{63}$$

By choose $y = n_i/|n_i|$, we see that $\phi^\circ(n_i) = 1$. Next, for $\lambda \in (0,1)$ and two adjacent normals $n_i, n_{i+1}$,

$$\phi^\circ(n_i\lambda + n_{i+1}(1-\lambda)) = \max\{n_i \cdot y\lambda + n_{i+1} \cdot y(1-\lambda) : \max_{n_j \in \mathcal{N}} \{n_j \cdot y\} = 1\}. \tag{64}$$

The maximizing $y$ satisfies $n_i \cdot y = n_{i+1} \cdot y = 1$. Therefore, $\phi^\circ(n_i\lambda + n_{i+1}(1-\lambda)) = \lambda + (1-\lambda) = 1$.

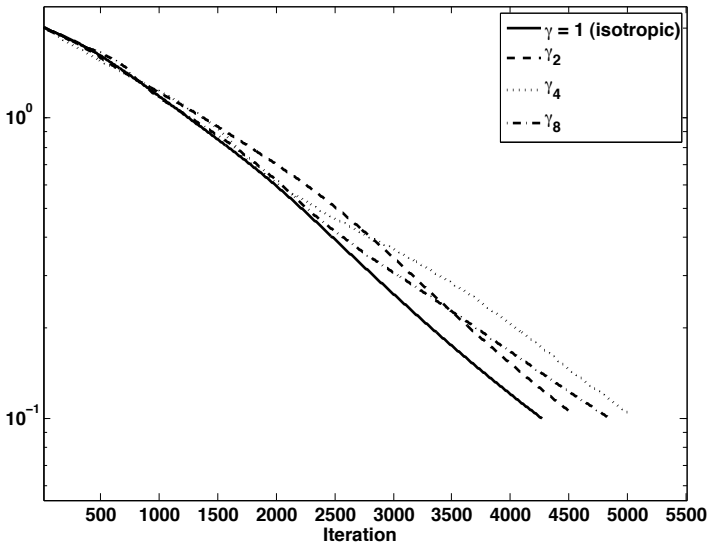


Figure 5: Plot of $\|\nabla u - d\|$ in a log-scale over iterations in the inverse scale space variable $s$.

*Proposition* 5. For a polyhedral norm $\phi(x) = \max_{n_i \in \mathcal{N}}\{n_i \cdot x\}$, the Wulff shape is the polygon with vertices $\mathcal{N}$.

Next we describe the Wulff shape for smooth norms. Define a smooth norm as per (43): $\phi(x) = \gamma(\theta_x)\|x\|$, where $\theta_x = \tan^{-1}(x_2/x_1)$. Then, the dual norm of $\phi$ is

$$\begin{aligned}\phi^\circ(x) &= \max\{x \cdot y : \gamma(\theta_y)\|y\| = 1\} \\ &= \max\{\|x\|\|y\|\cos(\theta_x - \theta_y) : \|y\|\gamma(\theta_y) = 1\} \\ &= \max_{\theta_y}\left\{\frac{\|x\|\cos(\theta_x - \theta_y)}{\gamma(\theta_y)}\right\}.\end{aligned}$$

If we write $\phi^\circ(x) = \gamma^*(\theta_x)\|x\|$, we have

$$\gamma^*(\theta_x) = \max_{\theta_y}\left\{\frac{\cos(\theta_x - \theta_y)}{\gamma(\theta_y)}\right\}. \tag{65}$$

Assuming $\gamma(\theta_y) \neq 0$ and smooth, the maximizer $\theta_y^*$ can be characterized by calculus:

$$\tan(\theta_x - \theta_y^*) = \frac{\gamma'(\theta_y^*)}{\gamma(\theta_y^*)}. \tag{66}$$

Furthermore, solving the differential equation for $\gamma(\theta_y^*)$ gives

$$\frac{\cos(\theta_x - \theta_y^*)}{\gamma(\theta_y^*)} = \frac{1}{\gamma(\theta_x)}. \tag{67}$$

Therefore, $\gamma^*(\theta_x) = 1/\gamma(\theta_x)$. We summarize the results in the following proposition.

*Proposition* 6. For a smooth norm $\phi(x) = \gamma(\theta_x)\|x\|$,

$$\partial\mathcal{W} = \{x : \|x\| = \gamma(\theta_x)\}.$$

## References


[ATW93] Fred Almgren, Jean E. Taylor, and Lihe Wang. Curvature-driven flows: a variational approach. *SIAM J. Control Optim.*, 31(2):387–438, 1993.

[BGOX06] Martin Burger, Guy Gilboa, Stanley Osher, and Jinjun Xu. Nonlinear inverse scale space methods. *Commun. Math. Sci.*, 4(1):179–212, 2006.

[Brè67] L. M. Brègman. A relaxation method of finding a common point of convex sets and its application to the solution of problems in convex programming. *Ž. Vyčisl. Mat. i Mat. Fiz.*, 7:620–631, 1967.

[BV04] Stephen Boyd and Lieven Vandenberghe. *Convex optimization*. Cambridge University Press, Cambridge, 2004.

[CDK95] Francine Catté, Françoise Dibos, and Georges Koepfler. A morphological scheme for mean curvature motion and applications to anisotropic diffusion and motion of level sets. *SIAM J. Numer. Anal.*, 32(6):1895–1909, 1995.

[CGG91] Yun Gang Chen, Yoshikazu Giga, and Shun'ichi Goto. Uniqueness and existence of viscosity solutions of generalized mean curvature flow equations. *J. Differential Geom.*, 33(3):749–786, 1991.

[Cha04] Antonin Chambolle. An algorithm for mean curvature motion. *Interfaces Free Bound.*, 6(2):195–218, 2004.

[DDE05] Klaus Deckelnick, Gerhard Dziuk, and Charles M. Elliott. Computation of geometric partial differential equations and mean curvature flow. *Acta Numer.*, 14:139–232, 2005.

[EO04] Selim Esedoḡlu and Stanley J. Osher. Decomposition of images by the anisotropic Rudin-Osher-Fatemi model. *Comm. Pure Appl. Math.*, 57(12):1609–1626, 2004.

[ES91] L. C. Evans and J. Spruck. Motion of level sets by mean curvature. I. *J. Differential Geom.*, 33(3):635–681, 1991.

[GBO09] Tom Goldstein, Xavier Bresson, and Stanley Osher. Geometric applications of the split bregman method: Segmentation and surface reconstruction. Technical report, UCLA, ftp://ftp.math.ucla.edu/pub/camreport/cam09-06.pdf, July 2009.

[Gig06] Yoshikazu Giga. *Surface evolution equations*, volume 99 of *Monographs in Mathematics*. Birkhäuser Verlag, Basel, 2006. A level set approach.

[GO09] Tom Goldstein and Stanley Osher. The split Bregman method for $L1$-regularized problems. *SIAM J. Imaging Sci.*, 2(2):323–343, 2009.

[Gur93] Morton E. Gurtin. *Thermomechanics of evolving phase boundaries in the plane*. Oxford Mathematical Monographs. The Clarendon Press Oxford University Press, New York, 1993.

[MBO94] Barry Merriman, James K. Bence, and Stanley J. Osher. Motion of multiple functions: a level set approach. *J. Comput. Phys.*, 112(2):334–363, 1994.

[NP07] Matteo Novaga and Maurizio Paolini. Nonuniqueness for crystalline curvature flow. *Math. Models Methods Appl. Sci.*, 17(8):1307–1315, 2007.

[Obe04] Adam M. Oberman. A convergent monotone difference scheme for motion of level sets by mean curvature. *Numer. Math.*, 99(2):365–379, 2004.

[OBG+05] Stanley Osher, Martin Burger, Donald Goldfarb, Jinjun Xu, and Wotao Yin. An iterative regularization method for total variation-based image restoration. *Multiscale Model. Simul.*, 4(2):460–489 (electronic), 2005.

[OS88] Stanley Osher and James A. Sethian. Fronts propagating with curvature-dependent speed: algorithms based on Hamilton-Jacobi formulations. *J. Comput. Phys.*, 79(1):12–49, 1988.

[ROF92] Leonid Rudin, Stanley Osher, and Emad Fatemi. Reconstruction and enhancement of signals using nonlinear non-oscillatory variational methods. *Phys. D*, 60(1-4):259–268, 1992.

Department of Mathematics, Simon Fraser University
*E-mail address*: aoberman@sfu.ca

Department of Mathematics, University of California, Los Angeles
*E-mail address*: sjo@math.ucla.edu

Department of Mathematics, University of California, Los Angeles
*E-mail address*: rrtakei@ucla.edu

Department of Mathematics, University of Texas, Austin
*E-mail address*: ytsai@math.utexas.edu